J. Fluid Mech. (1974), *vol.* 65, *part* 4, *pp.* 625–645
Printed in Great Britain

Transition to time-dependent convection

By R. M. CLEVER
Science Applications, Inc., El Segundo, California 90245

AND F. H. BUSSE
Department of Planetary and Space Sciences, University of California, Los Angeles

(Received 20 December 1973)

Steady solutions in the form of two-dimensional rolls are obtained for convection in a horizontal layer of fluid heated from below as a function of the Rayleigh and Prandtl numbers. Rigid boundaries of infinite heat conductivity are assumed. The stability of the two-dimensional rolls with respect to three-dimensional disturbances is analysed. It is found that convection rolls are unstable for Prandtl numbers less than about 5 with respect to an oscillatory instability investigated earlier by Busse (1972) for the case of free boundaries. Since the instability is caused by the momentum advection terms in the equations of motion the Rayleigh number for the onset of instability increases strongly with Prandtl number. Good agreement with various experimental observations is found.

1. Introduction

In recent years convection in a layer of fluid heated from below has become the principal example for the development of turbulence from a simple static state by way of discrete transitions. Among the various transitions the transition to oscillatory convection plays a special role since it introduces time dependence. Although the oscillatory instability occurs at relatively low Rayleigh numbers for Prandtl numbers of the order one or less, until recently it has not been investigated as intensively as the transition to bimodal convection. Experimentally as well as theoretically convection in a high Prandtl number fluid is easier to investigate, and it is for this reason that the transition to bimodal convection has been studied in considerable detail (Busse 1967; Krishnamurti 1970*a*; Busse & Whitehead 1971). Recently a number of experiments (Willis & Deardorff 1970; Krishnamurti 1970*b*, 1974) have shed light on the onset of time-dependent convection at low Prandtl numbers and the first rigorous theory on oscillatory convection was presented by Busse (1972) for the case of stress-free boundaries. Since in general the experiments were performed with rigid boundaries a direct comparison between observations and theoretical predictions has not been possible. In particular, the question of whether or not the linear stability analysis is capable of quantitatively describing the properties of the observed oscillations has remained unanswered. One of the motivations

for this paper is to fill this gap by extending the analysis of Busse (1972) to the more realistic case of rigid boundaries.

The extension of the theory of oscillations to rigid boundaries does not merely involve quantitative aspects. In contrast to other properties of convection the mechanism of the oscillatory instability is profoundly altered by the presence of rigid boundaries. It was pointed out by Busse (1972) that the occurrence of oscillations is connected with the appearance of vertical vorticity, which vanishes in the case of steady convection rolls. The role of the vertical vorticity differs significantly between the cases of rigid and free boundaries. The latter case is distinguished by the property that a non-decaying component of homogeneous vertical vorticity corresponding to a rigid rotation of the layer is permitted by the boundary conditions. Indeed, it always had to be assumed implicitly in theories of convection with free boundaries that the mean vertical vorticity vanishes. In the case of rigid boundaries this is a consequence of the boundary conditions. In the limit when the horizontal wavenumber of the disturbance vanishes a mode of vertical vorticity with vanishing dissipation exists in the case of free boundaries. Hence the critical Rayleigh number R_t for the onset of oscillations corresponds to this limit. In the case of rigid boundaries the critical value R_t is considerably higher and corresponds to a finite value of the horizontal disturbance wavenumber.

In addition to the oscillatory instability we investigate other possible mechanisms of instability in this paper in order to present a complete stability analysis of convection rolls as a function of the Prandtl number and Rayleigh number. Although the other instabilities are well understood from the case of infinite Prandtl number (Busse 1967) and from the stability analysis at small amplitude (Busse 1971) their dependence at finite amplitudes and finite Prandtl numbers is of interest for comparison with experiments.

A major part of the numerical analysis presented in this paper is concerned with the steady two-dimensional solution as a function of the wavenumber α, the Rayleigh number R and the Prandtl number P. The steady solutions have to be calculated with sufficient accuracy in order that reliable results for the onset of instabilities can be obtained. The properties of the steady solutions are of interest in themselves, however. It has been an open problem in the theory of convection that the measured convective heat transport appears to be relatively independent of Prandtl number while the small amplitude theory of Schlüter, Lortz & Busse (1965) predicts a variation proportional to P^2 in the limit of small P. The present analytical results show that a rapid increase of the convective heat transport with Rayleigh number takes place at low Prandtl number as the Rayleigh number is increased beyond the critical value R_c. The heat transport will also be influenced by the onset of oscillations. This influence is likely to be small, however, and has not been investigated in the framework of the present linear analysis of oscillations.

The paper starts in § 2 with the derivation of the non-dimensional equations for the problem. The method of solution is outlined for the case of the nonlinear steady problem and for the case of the linear stability analysis. The results for the steady solution as a function of wavenumber, Prandtl number and Rayleigh

number are described in § 3. The results of the stability analysis are presented in § 4. Each of the four mechanisms of instability is discussed separately and as far as possible the results are related to observed evidence. Some concluding remarks are made in § 5.

2. Mathematical formulation of the problem

2.1. *Basic equations*

The mathematical description of steady convection and its instabilities will be based on the Boussinesq approximation of the equations of motion and the heat equation. Accordingly, all material properties are assumed to be constant with the exception of the density in the gravity term. We shall use a dimensionless description by introducing the layer thickness d, d^2/κ and $\Delta T/R$ as scales for length, time and temperature, respectively, where κ is the thermal diffusivity and ΔT is the temperature difference between the lower and upper boundary of the convection layer. The dimensionless equations for the velocity vector $\mathbf{v}$ and for the deviation θ from the temperature distribution in the static state are

$$\nabla . \mathbf{v} = 0, \tag{1}$$

$$\nabla^2 \mathbf{v} + \boldsymbol{\lambda}\theta - \nabla\Gamma = P^{-1}(\mathbf{v}.\nabla\mathbf{v} + \partial\mathbf{v}/\partial t), \tag{2}$$

$$\nabla^2\theta + R\boldsymbol{\lambda}.\mathbf{v} = \mathbf{v}.\nabla\theta + \partial\theta/\partial t. \tag{3}$$

The dependence of the problem on the physical conditions of the layer has been reduced to two dimensionless parameters: the Rayleigh number R and the Prandtl number P. These parameters are defined by

$$R = \gamma g \Delta T d^3/\nu\kappa, \quad P = \nu/\kappa,$$

where γ is the coefficient of thermal expansion, ν is the kinematic viscosity and g is the acceleration due to gravity. The unit vector $\boldsymbol{\lambda}$ denotes the vertical direction opposite to that of gravity. All terms which can be expressed as gradients in (2) have been included in $\nabla\Gamma$.

It is convenient to eliminate the equation of continuity from the problem by introducing the following general representation for the solenoidal velocity field:

$$\mathbf{v} = \boldsymbol{\delta}\phi + \boldsymbol{\epsilon}\psi, \tag{4}$$

where the operators $\boldsymbol{\delta}$ and $\boldsymbol{\epsilon}$ are defined by

$$\boldsymbol{\delta}\phi = \nabla \times (\nabla \times \boldsymbol{\lambda}\phi), \quad \boldsymbol{\epsilon}\psi = \nabla \times \boldsymbol{\lambda}\psi.$$

After operating with $\boldsymbol{\lambda}.\nabla\times(\nabla\times$ and $\boldsymbol{\lambda}.\nabla\times$ on the equation of motion (2), we obtain from (2) and (3) the following equations for the scalar variables ϕ, ψ and θ:

$$\nabla^4\Delta_2\phi - \Delta_2\theta = \frac{1}{P}\left\{\boldsymbol{\delta}.[(\boldsymbol{\delta}\phi + \boldsymbol{\epsilon}\psi).\nabla(\boldsymbol{\delta}\phi + \boldsymbol{\epsilon}\psi)] + \frac{\partial}{\partial t}\nabla^2\Delta_2\phi\right\}, \tag{5}$$

$$\nabla^2\Delta_2\psi = \frac{1}{P}\left\{\boldsymbol{\epsilon}.[(\boldsymbol{\delta}\phi + \boldsymbol{\epsilon}\psi).\nabla(\boldsymbol{\delta}\phi + \boldsymbol{\epsilon}\psi)] + \frac{\partial}{\partial t}\Delta_2\psi\right\}, \tag{6}$$

$$\nabla^2\theta - R\Delta_2\phi = [(\boldsymbol{\delta}\phi + \boldsymbol{\epsilon}\psi).\nabla]\theta + \partial\theta/\partial t, \tag{7}$$

where Δ_2 denotes the Laplacian with respect to the horizontal dimensions;

$$\Delta_2 = \partial_{xx}^2 + \partial_{yy}^2.$$

The boundary conditions at the rigid boundaries of the layer are given by

$$\phi = \partial_z \phi = \psi = \theta = 0 \quad \text{at} \quad z = \pm \tfrac{1}{2}.$$

For the condition on θ we have made the usual assumption that the thermal conductivity of the solid region adjacent to the convection layer by far exceeds the conductivity of the fluid.

It is well known that steady solutions of (5) and (7) with vanishing vertical vorticity, i.e. $\psi \equiv 0$, exist for $R > R_c \equiv 1708$ (Chandrasekhar 1961, p. 34). In the paper by Schlüter *et al.* (1965), which we shall refer to as SLB in the following, it was shown that among all possible solutions only the solutions in the form of two-dimensional rolls are stable at small values of $R - R_c$. It is the goal of the present paper to investigate the stability of convection rolls for finite values of $R - R_c$ in the case of low to moderate Prandtl numbers and thereby extend the analysis of Busse (1967), who investigated the special case of infinite Prandtl number. For this purpose the steady two-dimensional solutions corresponding to convection rolls need to be computed first. Following this a linear analysis of their stability with respect to infinitesimal disturbances will reveal the range of physically realizable two-dimensional convection rolls.

2.2. *The steady problem*

The case of steady two-dimensional convection rolls corresponds to solutions independent of x and t of (5) and (7) with (6) having only a vanishing solution with $\psi \equiv 0$. Accordingly, the equations for ϕ and θ reduce to

$$\partial_y (\nabla^4 \phi - \theta) = P^{-1} \{\partial_{yz}^2 \phi \partial_{yzzz}^4 \phi - \partial_{yy}^2 \phi \partial_{yzzz}^4 \phi + \partial_{yz}^2 \phi \partial_{yyyy}^4 \phi - \partial_{yy}^2 \phi \partial_{yyyz}^4 \phi\}, \tag{8}$$

$$\nabla^2 \theta - R \partial_{yy}^2 \phi = \partial_{yz}^2 \phi \partial_y \theta - \partial_{yy}^2 \phi \partial_z \theta. \tag{9}$$

We shall solve (8) and (9) numerically by using a Galerkin technique. For this purpose we expand θ and ϕ in terms of orthogonal functions:

$$\phi = \sum_{\lambda, \nu} a_{\lambda\nu} e^{i\lambda\alpha y} g_\nu(z) \equiv \sum_{\lambda, \nu} a_{\lambda\nu} \phi_{\lambda\nu}, \tag{10a}$$

$$\theta = \sum_{\lambda, \nu} b_{\lambda\nu} e^{i\lambda\alpha y} f_\nu(z) \equiv \sum_{\lambda, \nu} b_{\lambda\nu} \theta_{\lambda\nu}. \tag{10b}$$

The functions

$$g_\nu(z) = \begin{cases} \dfrac{\sinh(\beta_{\frac{1}{2}\nu} z)}{\sinh(\frac{1}{2}\beta_{\frac{1}{2}\nu})} - \dfrac{\sin(\beta_{\frac{1}{2}\nu} z)}{\sin(\frac{1}{2}\beta_{\frac{1}{2}\nu})} & \text{for } \nu \text{ even} \\ \dfrac{\cosh(\lambda_{\frac{1}{2}(\nu+1)} z)}{\cosh(\frac{1}{2}\lambda_{\frac{1}{2}(\nu+1)})} - \dfrac{\cos(\lambda_{\frac{1}{2}(\nu+1)} z)}{\cos(\frac{1}{2}\lambda_{\frac{1}{2}(\nu+1)})} & \text{for } \nu \text{ odd} \end{cases} \tag{11a}$$

and

$$f_\nu(z) = \sin[\nu\pi(z + \tfrac{1}{2})] \tag{11b}$$

satisfy the boundary conditions for ϕ and θ, respectively. The values β_ν and λ_ν are determined as the positive roots of

$$\coth \tfrac{1}{2}\beta - \cot \tfrac{1}{2}\beta = 0, \quad \tanh \tfrac{1}{2}\lambda + \tan \tfrac{1}{2}\lambda = 0$$

and are given in the book by Chandrasekhar (1961, p. 635).

The summation in expressions $(10a, b)$ runs through all integers $-\infty < \lambda < \infty$ ($a_{0\nu}$ is excluded), $1 \leqslant \nu < \infty$. The symmetry of the basic equations allows us to restrict ourselves to the case of a solution symmetric in y for which

$$a_{\lambda\nu} = a_{-\lambda\nu}, \quad b_{\lambda\nu} = b_{-\lambda\nu}.$$

In order to compute the unknown coefficients $a_{\lambda\nu}$ and $b_{\lambda\nu}$ it is necessary to truncate the representation $(10a, b)$ at a sufficiently high level. Hence, we choose a truncation parameter N such that all coefficients with

$$|\lambda| + \nu > N \tag{12}$$

are neglected. After substituting expansions $(10a, b)$ into (8) and (9), multiplying them by $\phi_{\kappa\mu}$ and $\theta_{\kappa\mu}$, respectively, and averaging over the fluid layer we obtain the following set of algebraic equations for the unknowns $a_{\lambda\nu}$ and $b_{\lambda\nu}$:

$$\left.\begin{aligned} I^{(1)}_{\kappa\mu\lambda\nu} a_{\lambda\nu} + I^{(2)}_{\kappa\mu\lambda\nu} b_{\lambda\nu} + P^{-1} I^{(3)}_{\kappa\mu\lambda\nu\rho\pi} a_{\lambda\nu} a_{\rho\pi} &= 0 \quad (13a) \\ I^{(4)}_{\kappa\mu\lambda\nu} b_{\lambda\nu} + R I^{(5)}_{\kappa\mu\lambda\nu} a_{\lambda\nu} + I^{(6)}_{\kappa\mu\lambda\nu\rho\pi} a_{\lambda\nu} b_{\rho\pi} &= 0 \quad (13b) \end{aligned}\right\} \quad |\kappa| + \mu \leqslant N.$$

The summation convention has been applied in (13). The calculation of the matrices $\mathbf{I}^{(n)}$ from the terms givenin (8) and (9) is straightforward. Using angular brackets to indicate an average over the fluid layer we can write, for example,

$$I^{(1)}_{\kappa\mu\lambda\nu} \equiv \langle \phi_{\kappa\mu} \partial_y \nabla^4 \phi_{\lambda\nu} \rangle.$$

Because the nonlinear terms in (8) and (9) are quadratic and include an odd number of z derivatives the complete set (13) contains a subset of equations in which only variables with even $\lambda + \nu$ are present. All solutions which exist close to the critical Rayleigh number are contained in this subset. Hence it is sufficient to restrict the analysis to the subset because the physical realization of a more general two-dimensional solution must be associated with an instability. The results of the stability analysis in §4 do not show any indication that a two-dimensional solution not contained in the subset could be realized.

Assuming that the truncation parameter N is an even integer we have $\frac{1}{2}N(N+1)$ equations to solve. Starting with a guessed solution, usually a solution for a lower value of the Rayleigh number, we use a $\frac{1}{2}N(N+1)$ dimensional Newton–Raphson iteration procedure to obtain the solution. Convergence of the iterative scheme is ensured by an appropriate choice of the relaxation parameter. Between 5 and 10 iterates are usually sufficient to obtain a converged solution.

A more serious problem is the convergence of the truncation approximation. The choice of the truncation parameter N is regarded as satisfactory if the coefficients with $|\lambda| + \nu > N$ make a negligible contribution to the solution. Following Busse (1967) the convective heat transport was chosen as a criterion for the approximation owing to its fairly sensitive dependence on the higher-order coefficients. The convergence of the convective heat transport was not monotonic in N but showed a slight overshoot of 2–3 % or more at moderate Prandtl number and subsequent decrease to convergence as N was increased further. At lower Prandtl number the overshoot was more pronounced; for $P = 0{\cdot}001$ and $R \simeq 2000$ the overshoot approached a factor of 2 or more. Accord-

ingly, the truncation approximation was regarded as satisfactory if the value of the convective heat transport decreased by 1–2 % or less as the truncation parameter was increased from $N-2$ to N. Calculations in a few representative cases with larger truncation values have shown that the heat-transport values calculated using this criterion should be within $\frac{1}{2}$–1 % of the exact value.

2.3. *The stability problem*

For the investigation of the stability of the steady two-dimensional solution we superimpose onto it arbitrary infinitesimal disturbances. If any disturbance with a growing time dependence exists, the steady solution is unstable; otherwise it will be regarded as stable. The equations for the disturbance field $\{\tilde{\phi}, \tilde{\psi}, \tilde{\theta}\}$ are obtained from (5), (6) and (7) by replacing ϕ, ψ and θ by $\phi+\tilde{\phi}$, $\tilde{\psi}$ and $\theta+\tilde{\theta}$, respectively and subtracting the equations for the steady solution $\{\phi, \theta\}$:

$$\nabla^4\Delta_2\tilde{\phi}-\Delta_2\tilde{\theta}=\frac{1}{P}\left\{\boldsymbol{\delta}.[(\boldsymbol{\delta}\tilde{\phi}+\boldsymbol{\epsilon}\tilde{\psi}).\nabla(\boldsymbol{\delta}\phi)+(\boldsymbol{\delta}\phi).\nabla(\boldsymbol{\delta}\tilde{\phi}+\boldsymbol{\epsilon}\tilde{\psi})]+\frac{\partial}{\partial t}\nabla^2\Delta_2\tilde{\phi}\right\}, \tag{14a}$$

$$\nabla^2\Delta_2\tilde{\psi}=\frac{1}{P}\left\{\boldsymbol{\epsilon}.[(\boldsymbol{\delta}\tilde{\phi}+\boldsymbol{\epsilon}\tilde{\psi}).\nabla(\boldsymbol{\delta}\phi)+(\boldsymbol{\delta}\phi).\nabla(\boldsymbol{\delta}\tilde{\phi}+\boldsymbol{\epsilon}\tilde{\psi})]+\frac{\partial}{\partial t}\Delta_2\tilde{\psi}\right\}, \tag{14b}$$

$$\nabla^2\tilde{\theta}-R\Delta_2\tilde{\phi}=(\partial^2_{yz}\tilde{\phi}-\partial_x\tilde{\psi})\,\partial_y\theta-(\Delta_2\tilde{\phi})\,\partial_z\theta+\partial^2_{yz}\phi\partial_y\tilde{\theta}-\partial^2_{yy}\phi\,\partial_z\tilde{\theta}+\partial\tilde{\theta}/\partial t. \tag{14c}$$

Because of the infinitesimal amplitude of the disturbances, those terms which are quadratic in the disturbance variables have been neglected. Although the system (14) of stability equations is linear in contrast to the equations for the steady solution, the analysis is complicated by the fact that solutions with arbitrary three-dimensional spatial dependence have to be considered. However, since (14) does not depend explicitly on x and t and the explicit dependence on y is periodic the general solution can be written as a sum of solutions which depend exponentially on x, y and t and which are multiplied by a function of y and z with the same periodicity as the steady solutions:

$$\tilde{\phi}=\Big(\sum_{\lambda,\nu}\tilde{a}_{\lambda\nu}e^{i\lambda\alpha y}g_\nu(z)\Big)\,e^{i(dy+bx)+\sigma t}, \tag{15a}$$

$$\tilde{\psi}=\Big(\sum_{\lambda,\nu}\tilde{c}_{\lambda\nu}e^{i\lambda\alpha y}f_\nu(z)\Big)\,e^{i(dy+bx)+\sigma t}, \tag{15b}$$

$$\tilde{\theta}=\Big(\sum_{\lambda,\nu}\tilde{b}_{\lambda\nu}e^{i\lambda\alpha y}f_\nu(z)\Big)\,e^{i(dy+bx)+\sigma t}. \tag{15c}$$

The functions $f_\nu(z)$ and $g_\nu(z)$ are given by expressions (11). The variable $\tilde{\psi}$ has been expanded in the same system of functions as $\tilde{\theta}$ since both satisfy the same boundary conditions.

Substitution of expansions (15) into (14) leads to equations for the unknowns $\tilde{a}_{\lambda\nu}$, $\tilde{b}_{\lambda\nu}$ and $\tilde{c}_{\lambda\nu}$ when the same procedure as in the steady problem is used:

$$I^{(11)}_{\kappa\mu\lambda\nu}\tilde{a}_{\lambda\nu}+I^{(12)}_{\kappa\mu\lambda\nu}\tilde{b}_{\lambda\nu}+\frac{1}{P}\{I^{(13)}_{\kappa\mu\lambda\nu}\tilde{a}_{\lambda\nu}+I^{(14)}_{\kappa\mu\lambda\nu}\tilde{c}_{\lambda\nu}\}=\frac{\sigma}{P}I^{(15)}_{\kappa\mu\lambda\nu}\tilde{a}_{\lambda\nu},\quad |\kappa|+\mu\leqslant N, \tag{16a}$$

$$I^{(21)}_{\kappa\mu\lambda\nu}\tilde{c}_{\lambda\nu}+\frac{1}{P}\{I^{(22)}_{\kappa\mu\lambda\nu}\tilde{a}_{\lambda\nu}+I^{(23)}_{\kappa\mu\lambda\nu}\tilde{c}_{\lambda\nu}\}=\frac{\sigma}{P}I^{(24)}_{\kappa\mu\lambda\nu}\tilde{c}_{\lambda\nu},\quad |\kappa|+\mu\leqslant N, \tag{16b}$$

$$I^{(31)}_{\kappa\mu\lambda\nu}\tilde{b}_{\lambda\nu}+RI^{(32)}_{\kappa\mu\lambda\nu}\tilde{a}_{\lambda\nu}+I^{(33)}_{\kappa\mu\lambda\nu}\tilde{a}_{\lambda\nu}+I^{(34)}_{\kappa\mu\lambda\nu}\tilde{c}_{\lambda\nu}+I^{(35)}_{\kappa\mu\lambda\nu}\tilde{b}_{\lambda\nu}=\sigma I^{(36)}_{\kappa\mu\lambda\nu}\tilde{b}_{\lambda\nu},\quad |\kappa|+\mu\leqslant N. \tag{16c}$$

The coefficient matrices $I^{(ij)}_{\kappa\mu\lambda\nu}$ follow from the corresponding terms in (14). The matrices generated by the advection terms have a somewhat complicated structure. The calculation, however, is straightforward, as, for example, the definition of $I^{(3)}_{\kappa\mu\lambda\nu}$ is

$$I^{(13)}_{\kappa\mu\lambda\nu} = -\sum_{\rho\pi} a_{\rho\pi} \langle \tilde{\phi}_{\kappa\mu} \boldsymbol{\delta} . \{ \boldsymbol{\delta} \tilde{\phi}_{\lambda\nu} . \nabla \boldsymbol{\delta} \phi_{\rho\pi} + \boldsymbol{\delta} \phi_{\rho\pi} . \nabla \boldsymbol{\delta} \tilde{\phi}_{\lambda\nu} \} \rangle .$$

The system (16) of linear homogeneous equations constitutes an eigenvalue problem for the eigenvalue σ. In order to apply the usual algebraic eigenvalue methods, the indices λ and ν, and κ and μ had to be combined to form single running subscripts. In addition the coefficients $\tilde{a}_{\lambda\nu}$, $\tilde{b}_{\lambda\nu}$ and $\tilde{c}_{\lambda\nu}$ were combined sequentially to form a single variable. The analysis of the eigenvalue problem (16) is further simplified by noticing that it separates into four subsystems. First, it is seen that equations for coefficients with even $\lambda+\nu$ and odd $\lambda+\nu$ separate. In each case the symmetry of the steady solution with respect to the y direction allows a further separation into solutions which are either symmetric or antisymmetric in y. It should be noticed that in all cases the coefficients $\tilde{c}_{\lambda\nu}$ have the opposite symmetry properties to the coefficients $\tilde{a}_{\lambda\nu}$ and $\tilde{b}_{\lambda\nu}$. In the following, all references to symmetry properties will be made with respect to the latter coefficients.

The primary objective of the analysis of problem (16) is to determine as a function of α and P the Rayleigh number at which the real part of the eigenvalue σ with largest real part vanishes. The corresponding eigenvector describes the disturbance leading to instability of the steady solution when the Rayleigh number passes through the marginal value. Even though the system (16) has been separated into four sybsystems the amount of computation for the determination of stability boundaries is still substantial because of the large number of parameters involved. For this reason only a few representative cases will be investigated. Fortunately the dependence of the eigenvalue σ on various parameters is smooth and interpolation formulae can be used successfully to reduce the cost of computation.

3. The steady solution

In describing the numerical results for steady convection rolls we shall concentrate on the convective heat transport, which not only is the parameter of primary physical interest but which also appears to characterize best the other aspects of convection. For example, viscous dissipation occurs at the same rate as the convective heat transport according to the average of (2) after it is multiplied by $\mathbf{v}$:

$$\langle \mathbf{v} . \boldsymbol{\lambda} \theta \rangle = \langle |\nabla \mathbf{v}|^2 \rangle .$$

A number of numerical studies of convection rolls have yielded results for the Nusselt number

$$Nu = 1 + \langle \mathbf{v} . \boldsymbol{\lambda} \theta \rangle / R$$

as a function of the Prandtl number and the horizontal wavenumber α. Most of the previous results have been obtained by finite-difference methods, which have been reviewed by Plows (1968) and Denny & Clever (1974). The Fourier

R	$\alpha = 2{\cdot}2$			$\alpha = 2{\cdot}6$			$\alpha = 3{\cdot}117$		
	$P = 7{\cdot}0$	$P = 0{\cdot}71$	$P = 0{\cdot}025$	$P = 7{\cdot}0$	$P = 0{\cdot}71$	$P = 0{\cdot}025$	$P = 7{\cdot}0$	$P = 0{\cdot}71$	$P = 0{\cdot}025$
2000	—	—	—	1·155	1·152	1·0206	1·214	1·212	1·0610
2500	1·295	1·289	—	1·424	1·418	1·159	1·478	1·475	1·262
3000	1·500	1·489	—	1·615	1·608	—	1·667	1·663	1·437
5000	1·969	1·948	—	2·060	2·056	—	2·112	2·116	—
10 000	2·473	2·468	—	2·557	2·581	—	2·618	2·661	—
20 000	2.930	2·995	—	3·030	3·136	—	3·119	3·258	—
30 000	3·203	3·346	—	3·323	3·511	—	3·440	3·662	—
50 000	3·580	3·848	—	3·730	4·050	—	3·894	4·245	—

TABLE 1. Nusselt number as a function of Rayleigh number, Prandtl number and wavenumber.

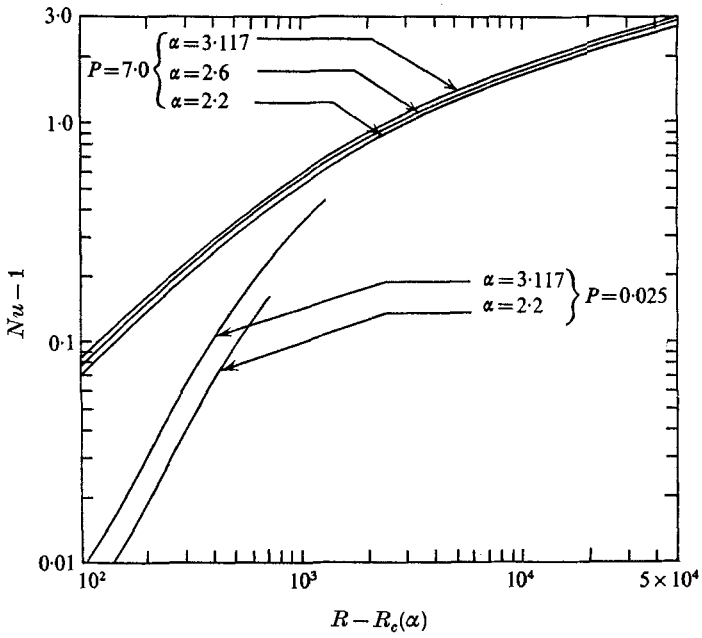

FIGURE 1. The wavenumber dependence of the convective heat transport. The values for $P = 0{\cdot}71$ are very close to those for $P = 7{\cdot}0$ as is evident from table 1.

expansion method used in the present analysis appears to circumvent some of the difficulties with the representation of the boundary conditions and extraction of the wall gradients in finite-difference methods. In addition, the numerical procedure used here for the steady solution is more easily extended to the investigation of the stability of convection rolls owing to the periodicity of the solutions in the horizontal co-ordinates. Representative Nusselt number results are given in table 1. Comparison with the results of Plows (1968) and the more recent work of Willis, Deardorff & Somerville (1972) shows good agreement between the two methods.

It is interesting to note that the convective heat transport at moderate Rayleigh numbers tends to increase with decreasing Prandtl number in contrast to the behaviour at Rayleigh numbers close to R_c, where the small amplitude results presented in SLB predict a monotonic decrease with decreasing P. At a Rayleigh number of about 4000, for $\alpha = 3{\cdot}117$, the heat transport in air already exceeds the heat transport in water by a small amount, which indicates a change in the role of the inertial terms at finite amplitude.

The wavenumber dependence of the Nusselt number given in figure 1 shows little variation with Rayleigh number. As in the case $P = \infty$, the maximum of the Nusselt number at a given Rayleigh number is attained for a wavenumber close to the critical value α_c.

The most interesting results of the present analysis are those obtained for the case of small Prandtl number, which has received little attention in the previous literature. This is partly caused by increasing numerical difficulties as the Prandtl number decreases. For this reason the range of Rayleigh numbers for which

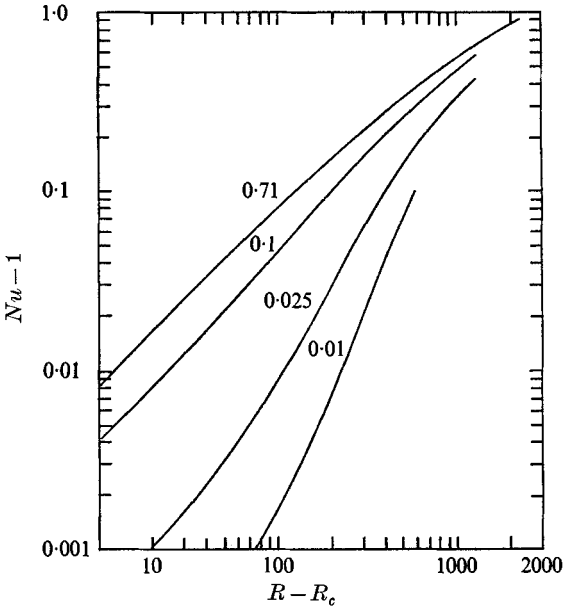

FIGURE 2. The dependence of the convective heat transport on the Rayleigh number for low Prandtl numbers (given on curves) at $\alpha = \alpha_c$. The figure indicates the convergence of the convective heat transport for different Prandtl numbers at higher Rayleigh numbers.

reliable results could be obtained decreased significantly even though values of the truncation parameter up to $N = 14$ or 16 were employed. This corresponds to the solution of 105 and 136 simultaneous nonlinear algebraic equations, respectively. On the other hand, calculations of the heat transport for two-dimensional convection do not correspond to physically realizable solutions beyond the second critical Rayleigh number R_t of instability, which also decreases significantly as P decreases as will be discussed in §4.4.

Even within these limitations the calculations shown in figures 2 and 3 tend to resolve, however, the old problem of the discrepancy between the theoretical prediction and observed dependence of the heat transport on the Prandtl number. While the small amplitude expansion results of SLB predict that convective heat transport should tend to zero like P^2 for a given small value of $R - R_c$, the present calculations indicate only a small influence of the Prandtl number on the heat transport for $R - R_c$ of order 1000. The finite amplitude results of the present analysis supplement the results of SLB in two important aspects. First, the range of $R - R_c$ for which the small amplitude result is applicable decreases rapidly with decreasing Prandtl number for $P \lesssim 0{\cdot}71$. Second, the dependence of the heat transport on $R - R_c$ beyond the range of validity of the small amplitude results shows a pronounced change as the Prandtl number is decreased below the value 0·71. This is shown in figure 3, where instead of continuing to fall below the line of constant $(Nu - 1)/(R - R_c)$ as suggested by the small amplitude results, the convective heat transport exceeds that value in order to increase rapidly until it nearly matches the heat transport of high

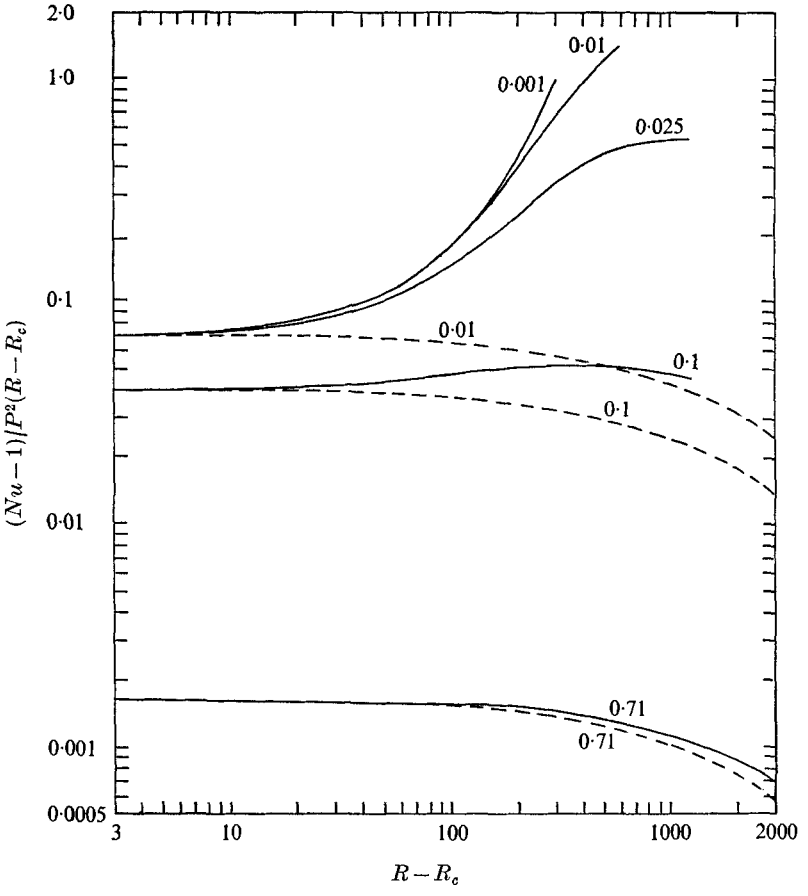

FIGURE 3. The convective heat transport scaled with $P^2(R-R_c)$. The curves indicate the qualitative difference between low Prandtl number cases and the case $P = 0{\cdot}71$, which is representative for higher Prandtl numbers. – – –, results derived from the small amplitude expansion in SLB. All curves are calculated for $\alpha = 3{\cdot}117$.

Prandtl number convection. As shown in figure 2 the P^2 decay of the convective heat transport at low Prandtl number is nearly offset when the Rayleigh number reaches a value of order 3000. Thus the heat transport becomes relatively independent of the Prandtl number at moderate Rayleigh numbers in agreement with experimental findings.

We interpret this interesting behaviour of the heat transport as the opposing effects of the nonlinear terms in the equation of motion and the heat equation. At moderate and large Prandtl numbers, when the momentum advection term is negligible in comparison with the heat advection term, the latter limits the increase of the convective heat transport. This saturation effect is primarily caused by the fact that the temperature fluctuation θ cannot exceed the prescribed temperature difference between the boundaries. At low Prandtl numbers, when the momentum advection term is much stronger, it shows the opposite effect. The inertia of the velocity field allows the convective heat transport to

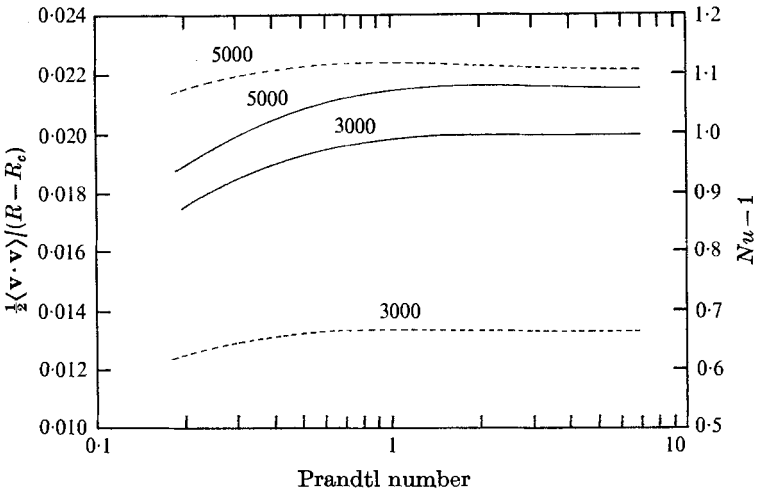

FIGURE 4. The dependence of the kinetic energy $\frac{1}{2}\langle \mathbf{v}\cdot\mathbf{v}\rangle$ on the Prandtl number for different Rayleigh numbers in the case $a = a_c$. For comparison the Nusselt number has been plotted (dashed lines).

become more effective and only at higher Rayleigh numbers does the limiting thermal factor become noticeable.

We have limited the discussion in this section to the convective heat transport although it comprises only a fraction of the numerical results obtained from the calculations. The kinetic energy of the convective velocity field is another physical quantity of interest. In the dimensionless form used in this paper it shows a dependence on the Prandtl number which is rather similar to that of the heat transport. This is evident from figure 4, which describes the kinetic energy in the case of the critical wavenumber a_c. For Prandtl numbers larger than unity the kinetic energy is essentially independent of the Prandtl number. At moderate Rayleigh numbers it exhibits a very slight maximum at about $P = 2$, which is somewhat larger than the Prandtl number at which the maximum heat transport occurs.

4. Stability boundaries for steady convection rolls

For a complete stability analysis the four subsets of the set (16) of equations corresponding to four different symmetries of the stability problem must be investigated for all values of the disturbance wavenumber parameters b and d. This investigation is eased by prior knowledge of the properties of potentially unstable disturbances. Qualitative insight into various instabilities can be gained from the analytical results of the small amplitude expansion. At Rayleigh numbers close to the critical value the analytical results can also be used for a quantitative comparison, which has been helpful in checking the accuracy of the numerical program. While some of the analytical results can be found in SLB a more extensive review has been given by Busse (1971). The main result of the analytical study is that critical disturbances for which the real part of the growth

rate σ reaches a maximum correspond to $b = 0$ or $d = 0$. Test calculations with the numerical program have shown that this property is not limited to Rayleigh numbers close to R_c. In the following we shall discuss four different classes of disturbances which may cause instability. We note that they do not all correspond to different subsets of the stability system (16). It turns out that disturbances with $\lambda + \nu$ odd and antisymmetric dependence on y were never found to have growing time dependence, at least not in the R, α, P region where all disturbances with $\lambda + \nu$ even or symmetric y dependence have negative real parts. In general, disturbances of certain symmetry were principally investigated in those regions where no growing disturbances of different symmetry had been found.

Complete stability regions in the R, α plane for steady rolls have been drawn in three representative cases, corresponding to the Prandtl numbers of water, air and mercury. Since the results for the case $P = \infty$ are known from previous work and since additional graphs have been given for the onset of the oscillatory instability, we feel that sufficient information is provided to give a fairly complete picture of the general stability behaviour of convection rolls.

4.1. *The cross-roll instability*

The cross-roll disturbances correspond to the case $d = 0$, $\lambda + \nu$ odd and symmetric y dependence. The name of these disturbances is derived from the property that at small Rayleigh number they tend to replace steady rolls with a wavenumber α sufficiently different from the critical value α_c with more nearly optimally adjusted convection rolls. The strongest growing cross-roll disturbances are characterized for this reason by a wavenumber b which is close to α_c. The fact that a perpendicular direction is favoured for the disturbance roll indicates that the stabilizing effects exerted by the steady roll are minimized at this angle. At high Rayleigh number the cross-roll disturbances change their character somewhat in that they become strongest in the thermal boundary layers. In this case the cross-roll instability leads to a transition to bimodal convection. Since the cross-roll instability has been investigated theoretically (Busse 1967) and experimentally (Busse & Whitehead 1971) in detail in the case of high Prandtl number we shall restrict the discussion to the influence of changing the Prandtl number. In general the momentum advection terms, which are proportional to P^{-1}, produce a stabilizing influence. This fact, which is already evident in the analytical results of Busse (1971), is found to hold even for large Rayleigh number. Also it is influenced by an increase in the heat transport, which tends to stabilize the thermal boundary layers according to an argument presented by Busse (1967). As a consequence the region of stable convection rolls is extended up to Rayleigh numbers of the order 5×10^4 in the case $P = 7{\cdot}0$ (figure 5) from the value $2{\cdot}3 \times 10^4$ in the case $P = \infty$. At lower Prandtl numbers the cross-roll instability loses importance since other mechanisms of instability appear to be more constraining.

Experimental observations of the stability of convection rolls to the cross-roll disturbance show the same Prandtl number dependence as do the present

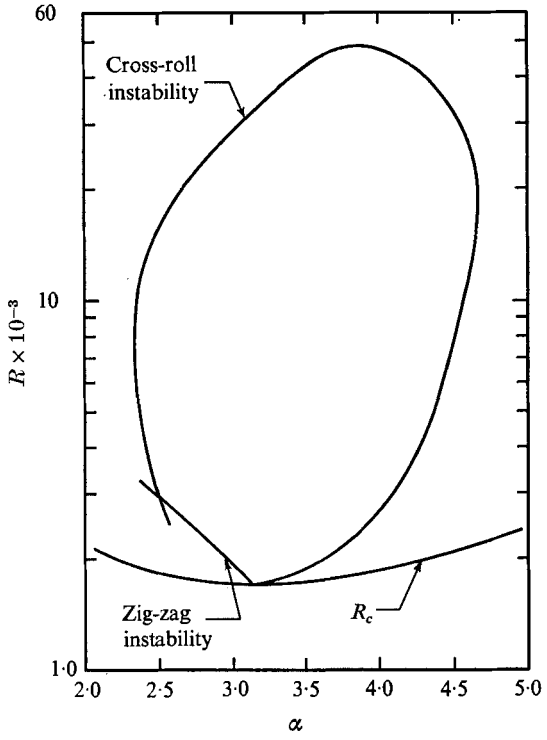

FIGURE 5. The stability of two-dimensional convection in a water layer ($P = 7{\cdot}0$). Convection rolls are stable in the closed region.

theoretical results. Krishnamurti (1970*a*, *b*) observes the second transition Rayleigh number to be essentially constant with decreasing Prandtl number (and also decreasing wavenumber) so far as the cross-roll instability is concerned. When the effects of a more pronounced decrease in wavenumber at lower Prandtl numbers are taken into account (Krishnamurti 1970*a*; Willis *et al.* 1972) the value of the Rayleigh number at which the transition to bimodal convection occurs in a water layer is consistent with the present investigation. The results of Chan (1972) also show the trend towards increased stability to the cross-roll disturbance at lower values of the Prandtl number. Chan shows the dependence of the cross-roll stability boundary on the wavenumber for $P \simeq 16$ and observes stable rolls up to a Rayleigh number of 3×10^4.

4.2. *The zig-zag instability*

The zig-zag disturbances cause the steady rolls to deform their boundaries in a zig-zag fashion thereby shortening the effective wavelength of the rolls. Accordingly, the zig-zag instability occurs when the wavenumber of the steady roll is too small. For convection at small amplitude it occurs when the wavenumber of the steady solution is less than the optimal value α_c. In the mathematical sense the zig-zag instability is formed out of disturbances with even $\lambda + \nu$ having antisymmetric y dependence with $d = 0$ and emerges out of a neutral disturbance

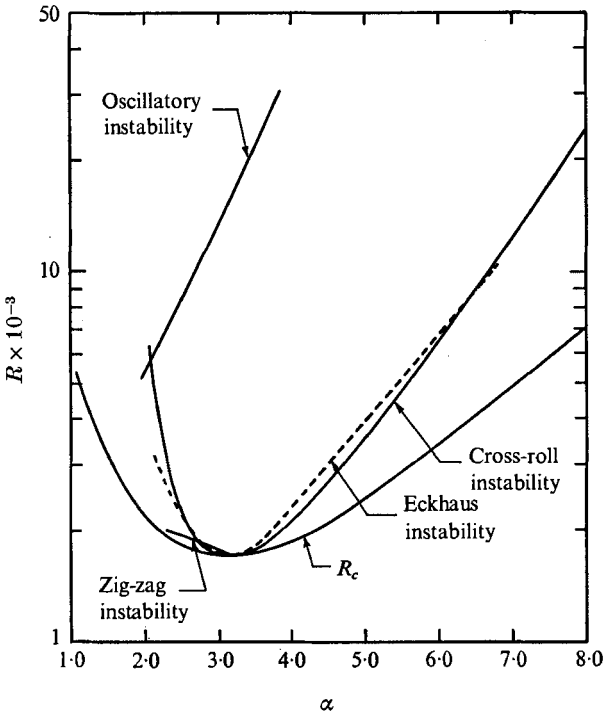

FIGURE 6. The stability of two-dimensional convection in an air layer ($P = 0{\cdot}71$). Convection rolls are stable for R below the oscillatory stability boundary and above either the Eckhaus or cross-roll boundary.

with vanishing growth rate in the limit of small b wavenumber. Again we can keep the description of this instability short since it has been investigated theoretically and experimentally in the high Prandtl number case (Busse 1967; Busse & Whitehead 1971).

As in the case of the cross-roll instability the momentum advection terms tend to have a stabilizing effect and in the case of air the zig-zag instability already becomes unimportant except in the region very close to R_c (figure 6). For mercury the instability was no longer noticeable within the accuracy of the calculations.

4.3. *The Eckhaus instability*

The Eckhaus instability corresponds to disturbances with $\lambda + \nu$ even, $b = 0$ and symmetric y dependence. It is the only instability of physical significance with $d \neq 0$ (except for asymmetric convection as caused, for example, by temperature-dependent properties). Eckhaus (1965) first discussed this two-dimensional instability in the context of the nonlinear Orr–Sommerfeld problem for Poiseuille flow. Although it represents a rather simple form of instability there appear to be no unambiguous experimental observations of it. This is mainly caused by the fact that convection experiments with controlled initial conditions are difficult to perform at low Prandtl numbers, where the Eckhaus mechanism becomes important. As was pointed out by Busse (1971) the Eckhaus

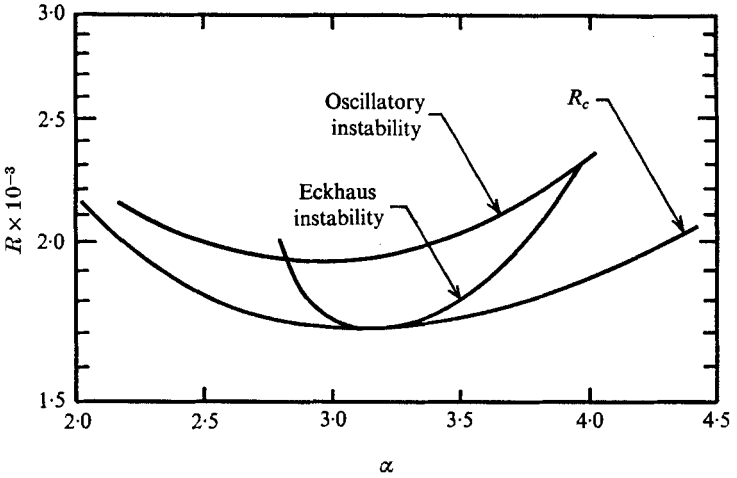

FIGURE 7. The stability of two-dimensional convection in a layer of mercury ($P = 0{\cdot}025$). Within the closed region convection rolls are stable.

instability replaces the cross-roll instability in limiting the wavenumber of physically realizable small amplitude convection for Prandtl numbers less than 1·1. The present numerical results confirm Busse's small amplitude results as is shown in figure 6. At higher Rayleigh numbers with $P = 0{\cdot}71$ the cross-roll instability still appears to have a slight edge over the Eckhaus mechanism. This property tends to vanish as the Prandtl number is further decreased and for mercury (figure 7) the appearance of the cross-roll instability is fully replaced by the Eckhaus instability.

4.4. *The oscillatory instability*

The oscillatory instability shares with the zig-zag instability the property that it corresponds to disturbances with $\lambda + \nu$ even, $d = 0$ and antisymmetric y dependence. While in the limit of small b wavenumber the zig-zag instability reduces to a neutral disturbance corresponding to a small shift of the roll pattern in the y direction, the oscillatory disturbance retains in the same limit a finite value of the vertical vorticity. In the limit $b = 0$ the vertical vorticity becomes independent of the horizontal co-ordinates and corresponds to a slight rotation of the steady convection pattern. Because of the presence of rigid boundaries this disturbance is highly damped as is evident in figure 8. This property is qualitatively changed in the case of free boundaries since instability is possible even in the limit of small b wavenumber although the growth rate becomes vanishingly small in this limit. This qualitative difference explains, however, why the critical Rayleigh number R_t for the onset of oscillations is much higher in the case of rigid boundaries than in the case of free boundaries.

A qualitative sketch of the instability is shown in figure 9. Instructive photographs of oscillatory convection rolls in air layers are shown in the paper by Willis & Deardorff (1970). The agreement between experimental findings and the present theoretical predictions is nearly perfect. In order to make a comparison

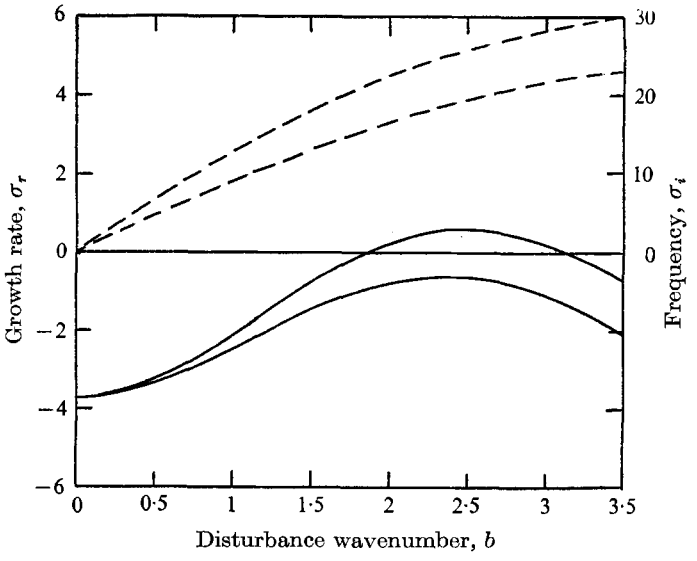

FIGURE 8. The dependence of σ and b for the oscillatory instability in the case $P = 0{\cdot}71$ and $\alpha = 2{\cdot}0$. The lower and the upper curves in the case of the real part of σ (solid lines) and in the case of the imaginary part (dashed lines) refer to $R = 5000$ and $R = 7000$, respectively.

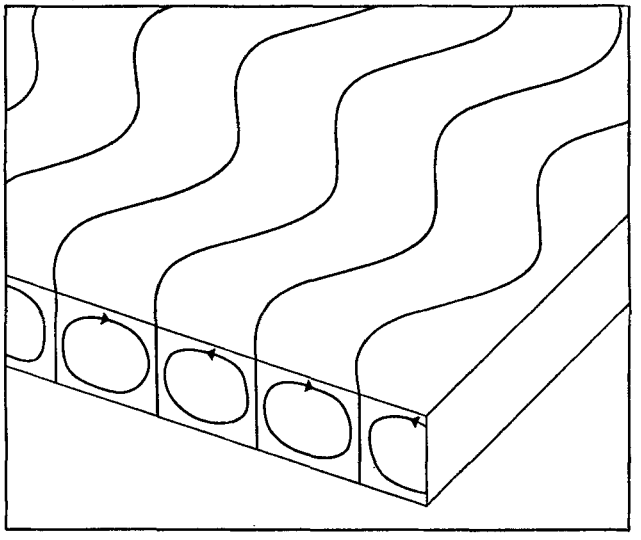

FIGURE 9. A qualitative sketch of oscillating convection rolls. The bending of the rolls propagates along the roll axis in time.

of the critical Rayleigh numbers R_t for the onset of oscillations the strong dependence of R_t on the wavenumber α has to be taken into account. A plot of the experimentally observed wavenumber dependence on the Rayleigh number for an air layer is given in the paper by Willis *et al.* (1972). When this is plotted on the stability diagram given in figure 6 a value of $R_t \simeq 6000$ is obtained which compares well with the value $R_t \simeq 5800$ observed by Willis & Deardorff (1970).

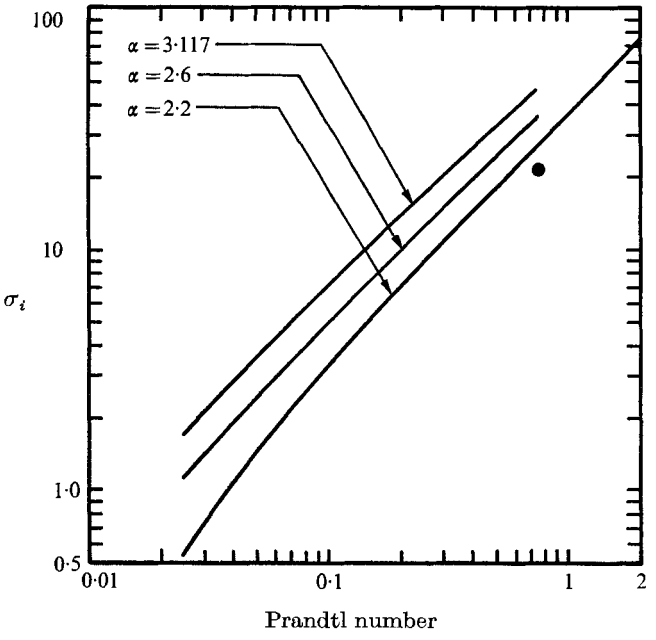

FIGURE 10. The frequency of the oscillatory disturbance in the case $\sigma_r = 0$ for different values of α (shown on curves). ●, experimental results of Willis & Deardorff (1970) for $R \approx 6000$ and $\alpha \approx 2{\cdot}2$.

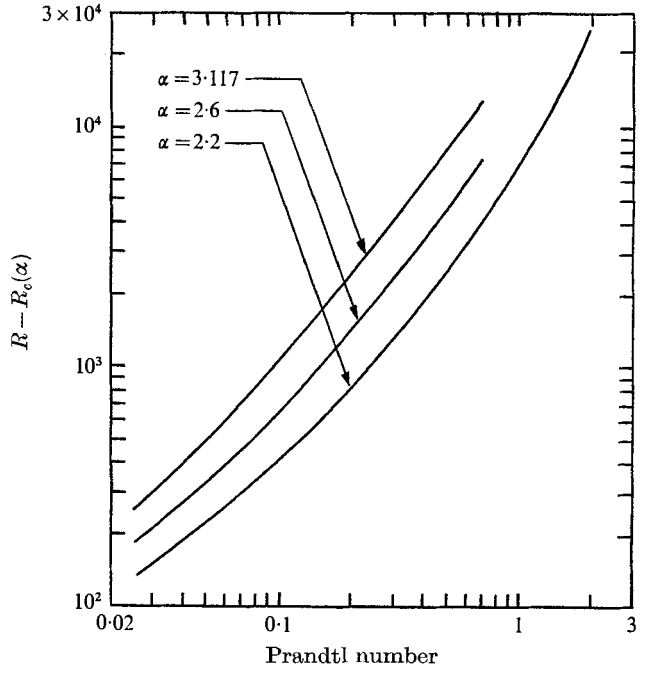

FIGURE 11. The critical Rayleigh number R_t for the onset of the oscillatory instability *vs.* the Prandtl number for different wavenumbers α (shown on curves).

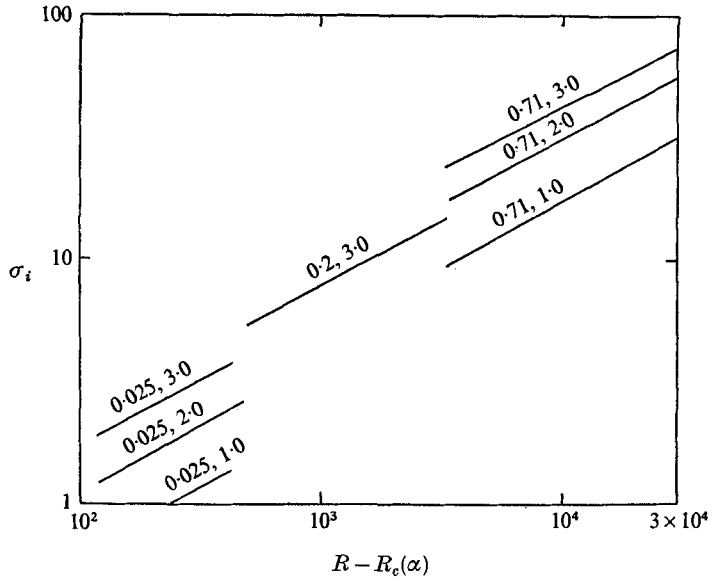

FIGURE 12. The frequency of the oscillatory disturbance as a function of the Rayleigh number. The numbers on the curves indicate the Prandtl number (first figure) and the wavenumber b. The dependence of σ_i on the wavenumber α is negligibly small.

The comparison for the frequency shows similar agreement. In figure 10 the frequency of oscillation at the onset of instability (figure 11) has been plotted as a function of the Prandtl number and wavenumber α. Figure 12 shows the dependence of σ_i on the b wavenumber at larger Rayleigh numbers. The good agreement between theory and experiment does not leave any doubt that they describe the same phenomenon.

In the case of mercury no direct visual observations have been possible and the comparison between theory and experiment is less satisfying. In a recent paper Krishnamurti (1974) reports that oscillations are first observed at $R \approx 2400$. This is somewhat higher than is indicated by the theoretical curve shown in figure 7 even if it is taken into account that the experimental wavenumber dependence on the Rayleigh number is not known owing to the lack of direct visual observations. This discrepancy may be caused either by the fact that finite oscillation amplitudes are required for the observations or the fact that the theoretical condition of infinite conductivity of the boundary is not sufficiently approximated in the experiment with mercury.

In the case of water no experimental observations of the oscillatory instability of convection rolls have been reported. This is in agreement with the present theoretical results that the cross-roll instability leading to bimodal convection sets in at lower Rayleigh numbers than does the oscillatory instability. For this reason the latter instability has not been drawn in figure 5. It is estimated that for Prandtl numbers less than about 5 the stability boundaries of the oscillatory and cross-roll instabilities intersect in the R, α plane.

5. Concluding remarks

A major conclusion to be drawn from the theory presented in this paper is the fact that the transition from steady convection to time-dependent convection depends strongly on the wavenumber α. The wavenumber is not an external parameter and may depend on numerous secondary influences in laboratory experiments. Nonlinear instability mechanisms induced by the side walls of the convection layer have been shown to change the wavenumber (Busse & Whitehead 1971) and the rate at which the Rayleigh number is increased in the convection experiment is likely to have a significant influence. Krishnamurti (1970*a*) has studied the experimental dependence on the wavenumber in the case of the transition to bimodal convection and has emphasized hysteresis effects. Since the oscillatory instability exhibits an even stronger dependence on the wavenumber, considerable variation in the transition to time-dependent convection has to be expected in different experiments.

The interesting feature of the oscillatory instability is the fact that it does not occur at Rayleigh numbers close to the critical value R_c. All other instabilities mentioned in this paper show stability boundaries converging at $R = R_c$. The property that the amplitude of motion has to exceed a finite value for the onset of oscillations is similar to the changing influence of the momentum advection term on the convective heat transport. In this case the amplifying influence becomes noticeable also only after a certain finite amplitude has been exceeded.

The fact that the oscillatory instability is caused by the momentum advection terms has been emphasized earlier (Busse 1972). The present results support this reasoning even though calculations have not been carried to very high Prandtl numbers. One may speculate whether oscillatory instabilities can be expected in the limit of infinite Prandtl number. While the heat equation seems to indicate that oscillations cannot be supported without the presence of the momentum advection terms a rigorous answer to this question has not been given.

The research reported in this paper was partly supported by the National Science Foundation under Grant GK-31246. A major portion of this work has been part of the Ph.D. dissertation submitted by one of the authors (RMC) in partial fulfillment of the requirements for the Ph.D. degree in Engineering at UCLA.

REFERENCES

Busse, F. H. 1967 On the stability of two-dimensional convection in a layer heated from below. *J. Math. & Phys.* **46**, 140–150.

Busse, F. H. 1971 Stability regions of cellular fluid flow. *Proc. IUTAM-Symp., Herrenalb*, 1969: *Instability of Continuous Systems* (ed. H. Leipholz), pp. 41–47. Springer.

Busse, F. H. 1972 The oscillatory instability of convection rolls in a low Prandtl number fluid. *J. Fluid Mech.* **52**, 97–112.

Busse, F. H. & Whitehead, J. A. 1971 Instabilities of convection rolls in a high Prandtl number fluid. *J. Fluid Mech.* **47**, 305–320.

CHAN, G. L. 1972 Experimental investigations of cellular convection in low and moderate Prandtl number fluids. M.S. thesis, School of Engineering, University of California, Los Angeles.

CHANDRASEKHAR, S. 1961 *Hydrodynamic and Hydromagnetic Stability*. Oxford: Clarendon Press.

DENNY, V. E. & CLEVER, R. M. 1974 Comparisons of Galerkin and finite-difference methods in highly nonlinear thermally driven flows. *J. Comp. Phys.* In press.

ECKHAUS, W. 1965 *Studies in Nonlinear Stability Theory*. Springer.

KRISHNAMURTI, R. 1970*a* On the transition to turbulent convection. Part 1. The transition from two- to three-dimensional flow. *J. Fluid Mech.* **42**, 295–307.

KRISHNAMURTI, R. 1970*b* On the transition to turbulent convection. Part 2. The transition to time-dependent flow. *J. Fluid Mech.* **42**, 309–320.

KRISHNAMURTI, R. 1974 Some further studies on the transition to turbulent convection. *J. Fluid Mech.* **60**, 285–303.

PLOWS, W. H. 1968 Some numerical results for two-dimensional steady laminar Bénard convection. *Phys. Fluids*, **11**, 1593–1599.

SCHLÜTER, A., LORTZ, D. & BUSSE, F. 1965 On the stability of steady finite amplitude convection. *J. Fluid Mech.* **23**, 129–144.

WILLIS, G. E. & DEARDORFF, J. W. 1970 The oscillatory motions of Rayleigh convection. *J. Fluid Mech.* **44**, 661–672.

WILLIS, G. E., DEARDORFF, J. W. & SOMERVILLE, R. C. J. 1972 Roll-diameter dependence in Rayleigh convection and its effect upon the heat flux. *J. Fluid Mech.* **54**, 351–367.